Modeling and Variables Estimation of a Two-phase Stepper Motor by using Extended Kalman Filter

Rafik Salloum, Mohammad Reza Arvan, Bijan Moaveni

Abstract— This paper presents the detailed mathematical and Simulink® model of a two-phase stepper BLDC motor in the machine variables, proving the rotor's position role in supplying the motor. Then an extended Kalman filter (EKF) is designed to estimate the motor state variables: stator currents, and the rotor position and velocity, on the basis of noisy measurements of stator currents, since it has a nonlinear function with time. The temperature change effects on the motor's performance are verified. Simulation results show that the motor's rotor position and velocity can be estimated in a satisfactory accuracy by the proposed method.

Keywords— BLDC motor, EKF, Estimation, Stepper motor.

1 INTRODUCTION

Existing trends in more electrification of automobiles indicate a further increase in deployment of electromechanical energy devices in coming years. Due to their high efficiency, long lifetime, and excellent servo control performance, permanent magnet brushless dc (BLDC) motors are now used extensively. Two-phase permanent magnet synchronous BLDC motors are commonly utilized as the stepper motors which are effectively utilized as direct drives and servos. In addition, the stepper motors usually operate in the open-loop configuration, especially when the load and inertia applied to the rotor are constant. The stepper motor rotates step-by-step by properly "energizing" the windings by supplying u_{as} and u_{bs}. However, the brushless dc motor requires a rotor position sensor with which commutation and current control are performed, such as resolvers and absolute encoders which increase cost, complexity and size of the motor and restrict its application [1]. Furthermore, as the application fields expand, the brushless dc motor is used in a special case where the motor cannot be provided with a position sensor. Many sensorless control methods which drive the brushless dc motors without position and speed sensors have been proposed. In [2], an approach for measuring the speed of a BLDC depends on measuring the frequency of the voltage between two phases of the motor was presented. While, in [3], a current feedback was used to estimate the rotor position of a stepper motor, and a filter was implemented in order to compensate the position estimation error. A current injection based method was proposed in [4] to estimate and correct the error of position estimation in BLDC motor.

In this paper, the open loop work case and the sensorless case by using the continuous time extended Kalman filter are considered for a two-phase brushless dc motor, like that shown in Fig. 1.

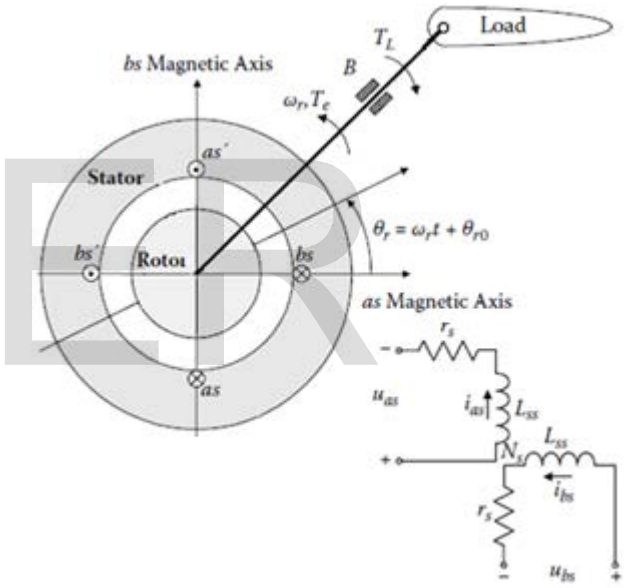

Fig. 1. Two-phase symmetrical BLDC motor.

One of sensorless control methods is the Extended Kalman Filter (EKF) sensorless control. It appears to be a viable and computationally efficient candidate for the on-line estimation of the speed and rotor position. This is possible since a mathematical model, describing the motor dynamics is sufficiently well known. The terminal quantities like voltages and currents can be measured easily and are suitable for the determination of the rotor position and speed in an indirect way. In [5], a discrete EKF approach was applied to estimate the position and speed of a permanent magnet synchronous motor. In addition to estimate the motor variables by discrete EKF, it was employed with a position feedback controller to compensate the load variations in [6], and applied to a stepper motor driver that works with long cables in [7].

In this paper, simulations are carried out to show the performance of the proposed continuous time EKF estimator and compare it with the theoretical one.

• *Rafik Salloum is currently pursuing PhDdegree program in electric engineering in Iran University of Science and Technology, Iran, PH-02177562346. E-mail: rafsal@mail.iust.ac.ir*

Nomenclatures of the used symbols are tabulated at the end of this paper.

2 MOTOR MODELLING

For stepper motors, the electrical angular velocity and displacement are found using the number of rotor tooth RT, i.e. $\omega_r = RT\ \omega_{rm}$, and $\theta_r = RT\ \theta_{rm}$. Where θ_r is the angular displacement of the rotor and it is defined as follows: $\omega_r = d\theta_r/dt$.

A 2-phase machine with identical stator windings is commonly considered a symmetrical 2-phase induction machine, the a_s and b_s windings are assumed to have N_s equivalent turns with resistance r_s [8]. To derive the governing equations for the studied motor, the stator circuitry-electromagnetic dynamics should be described, then the mechanical behavior should be modeled, and the electromagnetic torque is expressed.

Consider the motor shown in Fig. 1. Using Kirchhoff's voltage law, the voltage equations expressed in the machine variables may be written as follows:

$$u_{as} = r_s i_{as} + \frac{d\psi_{as}}{dt} \quad (1)$$

$$u_{bs} = r_s i_{bs} + \frac{d\psi_{bs}}{dt} \quad (2)$$

Where the flux linkages per second are expressed as:

$$\psi_{as} = L_{asas} i_{as} + L_{asbs} i_{bs} + \psi_{asm} \quad (3)$$

$$\psi_{bs} = L_{bsas} i_{as} + L_{bsbs} i_{bs} + \psi_{bsm} \quad (4)$$

The stator self-inductances are identical, i.e. $L_{asas} = L_{bsbs} = L_{ss}$. The stator windings are displaced by 90 electrical degrees. Hence, the mutual inductances between the stator windings are L_{asbs}=L_{bsas}=0. In addition, the flux linkages: ψ_{asm} and ψ_{bsm} present the amplitude of the flux linkages established by the permanent magnet as viewed from the stator phase windings, which are functions of the number of the rotor tooth and displacement.

$$\psi_{asm} = \psi_m.cos(RT\theta_{rm})\ ;\ \psi_{bsm} = \psi_m.sin(RT\theta_{rm})$$

Thus, (3) and (4) can be rewritten as follows:

$$\psi_{as} = L_{ss} i_{as} + \psi_m.\cos(RT\theta_{rm}) \quad (5)$$

$$\psi_{bs} = L_{ss} i_{bs} + \psi_m.\sin(RT\theta_{rm}) \quad (6)$$

Then, (1) and (2) yield:

$$u_{as} = r_s i_{as} + L_{ss}\frac{di_{as}}{dt} - RT\psi_m\omega_{rm}\sin(RT\theta_{rm}) \quad (7)$$

Therefore,

$$u_{bs} = r_s i_{bs} + L_{ss}\frac{di_{bs}}{dt} + RT\psi_m\omega_{rm}\cos(RT\theta_{rm}) \quad (8)$$

$$\frac{di_{as}}{dt} = -\frac{r_s}{L_{ss}} i_{as} + \frac{RT\psi_m}{L_{ss}}\omega_{rm}.\sin(RT\theta_{rm}) + \frac{1}{L_{ss}}u_{as} \quad (9)$$

$$\frac{di_{bs}}{dt} = -\frac{r_s}{L_{ss}} i_{bs} - \frac{RT\psi_m}{L_{ss}}\omega_{rm}.\cos(RT\theta_{rm}) + \frac{1}{L_{ss}}u_{bs} \quad (10)$$

The expression for the electromagnetic torque developed by the motor is obtained by deriving the co-energy:

$$W_c = 0.5(L_{ss} i_{as}^2 + L_{ss} i_{bs}^2) + \psi_m i_{as}\cos(RT\theta_{rm}) + \psi_m i_{bs}\sin(RT\theta_{rm}) + W_{PM} \quad (11)$$

$$T_e = \frac{\partial W_c}{\partial \theta_{rm}} = RT\psi_m[-i_{as}sin(RT\theta_{rm}) + i_{bs}cos(RT\theta_{rm})] \quad (12)$$

Newton's second law yields:

$$J\frac{d^2\theta_{rm}}{dt^2} = T_e - B_m\omega_{rm} - T_L \quad (13)$$

Hence, the behavior of the motor's currents, rotor angular velocity, and displacement are described by the following equations set:

$$\begin{aligned}
\frac{di_{as}}{dt} &= -\frac{r_s}{L_{ss}} i_{as} + \frac{RT\psi_m}{L_{ss}}\omega_{rm}.sin(RT\theta_{rm}) + \frac{1}{L_{ss}}u_{as} \\
\frac{di_{bs}}{dt} &= -\frac{r_s}{L_{ss}} i_{bs} - \frac{RT\psi_m}{L_{ss}}\omega_{rm}.cos(RT\theta_{rm}) + \frac{1}{L_{ss}}u_{bs} \\
\frac{d\omega_{rm}}{dt} &= \frac{RT\psi_m}{J}[-i_{as}sin(RT\theta_{rm}) + i_{bs}cos(RT\theta_{rm})] - \frac{B_m}{J}\omega_{rm} - \frac{1}{J}T_L) \\
d\theta_{rm}/dt &= \omega_{rm}
\end{aligned} \quad (14)$$

These equations were used to implement the stepper motor Simulink® model in the equivalent s-domain, as illustrated in Fig. 2.

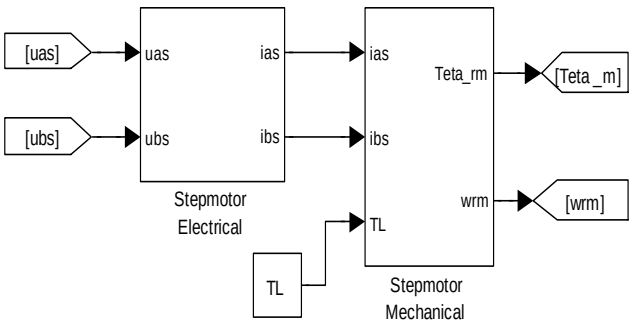

Fig. 2. Stepper motor Simulink model.

It's noted from the electromagnetic form illustrated in (12) that in order to get a balanced two-phase current sinusoidal set:

$$i_{as} = -\sqrt{2}i_s.\sin(RT\theta_{rm}) \text{ and } i_{bs} = \sqrt{2}i_s.\cos(RT\theta_{rm})$$

This produces the maximum torque form:

$T_e = \sqrt{2}RT\psi_m i_s$.

Consequently, the phase voltages u_{as} and u_{bs} should be supplied as functions of the rotor angular displacement in order to maximize the electromagnetic torque.

$$u_{as} = -\sqrt{2}u_s.\sin(RT\theta_{rm}) \text{ and } u_{bs} = \sqrt{2}u_s.\cos(RT\theta_{rm}).$$

However, to implement this supply, the angular displacement of motor's rotor should be known by one of the following methods:

1. Measuring the rotor angular displacement by using sensors like Hall sensors which are commonly used for this purpose.
2. Observing the rotor angle by using the induced emf or phase currents measurements.

Alternatively, to eliminate the need for sensors or observers (sensorless control), two solutions are available for stepper motors:

1- Stepper motors can operate in the open-loop configuration, particularly at low speeds and in steady-state operation, by supplying the phase voltages with frequency ωa. For example, without measuring θrm, one may supply the pulses:

$$u_{as} = -\sqrt{2}u_s.\text{sgn}(\sin(\omega_s t)) \text{ and } u_{bs} = \sqrt{2}u_s.\text{sgn}(\cos(\omega_s t - \frac{\pi}{2}))$$

2- Estimation of the motor's rotor angle and speed by using different algorithms, and this will be examined next in this paper by employing EKF.

3 EXTENDED KALMAN FILTER (EKF)

The extended Kalman filter algorithm is an optimal recursive estimation algorithm for nonlinear systems which is well explained in literature [9, 10]. It processes all available measurements regardless of their precision, to provide a quick and accurate estimate of the variables of interest, and also achieves a rapid convergence.

The main goal of using EKF is to estimate the motor's variables: stator currents, and the rotor's position and velocity, on the basis of noisy measurements of the stator currents.

The continuous time extended Kalman filter is applied to the continuous model of the stepper motor in the state space extracted in equations set (14) which is nonlinear due to the states product. Because the number of the parameters to be identified is four, a forth order parameter vector is defined as:

$\underline{x} = [i_{as}\ i_{bs}\ \omega_r\ \theta_r]^T$

In addition, define: $\underline{\mathbf{u}} = [u_{as}\ u_{bs}]^T$; $\underline{z} = [i_{as}\ i_{bs}]^T$

The EKF algorithm can be summarized as follows:

* **System model and measurement model:** Assuming a nonlinear system given by

$$\dot{x} = f(x,u,t) + G(t)w; \quad w(t) \sim (0,Q)$$
$$z = h(x,t) + v; \quad v(t) \sim (0,R)$$

* **Assumptions:** {w(t)} and {v(t)} are the system and measurement noises respectively, with covariances Q and R resp., and these noises are assumed to be white noise processes uncorrelated with x(0) and with each other.
* **Initialization:** The filter is initialized by $P(0) = P0$; $\hat{x}(0) = \underline{x_0}$
* **Estimate update:**

$$\dot{\hat{x}} = f(\hat{x},u,t) + K[z - h(\hat{x})]$$

* **Error covariance update:**

$$\dot{P} = A(\hat{x},t)P + PA^T(\hat{x},t) + GQG^T - PH^T(\hat{x},t)R^{-1}H(\hat{x},t)P$$

* **Kalman gain:**

$K = PH^T(\hat{x},t)R^{-1}$ with

$$A(x,t) = \frac{\partial f(x,u,t)}{\partial x}; \quad H(x,t) = \frac{\partial h(x,t)}{\partial x}$$

4 SIMULATION AND RESULTS ANALYSIS

The derived equations of the considered motor and its Simulink® model are applied for simulation. A Pacific Scientific stepper motor E24HSXS data [11], listed in Table 1, at temperature 20 °C are implemented into the EKF algorithm.

TABLE 1
MOTOR DATA AT 20 °C

Parameter	Value
V_{LL}	7.6 [V]
$i_{as_{max}} = i_{bs_{max}}$	7.4 [A]
J	0.0015 [Kg.m²]
r_s	0.43 [Ω]
L_{ss}	0.009 [H]
ψ_m	0.026 [N.m/A]
B_m	0.005 [N.m.sec/rad]

- The starting values of the estimations of the state vector and the parameter vector are set to zero-vectors, i.e.: $\hat{x}(0) = \underline{x_0} = 0$.

For the covariance matrix of the estimation error was set to identity: $P_0 = eye\ (4)$.

- In this application the measurement matrix H is linear: $H = \begin{bmatrix} 1 & 0 & 0 & 0 \\ 0 & 1 & 0 & 0 \end{bmatrix}$
- The measurement noise covariance matrix: $R = \begin{bmatrix} r^2 & 0 \\ 0 & r^2 \end{bmatrix}$ where r is the standard deviation of measurement noise. The diagonal elements of the measurement noise covariance matrix r were chosen according to the measurement error of the current sensors (0.7%) [12].

$r = 0.052$ A.

- The evaluation of the system noise covariance matrix is more complicated. It accounts for the model inaccuracy, system disturbances, and the measurement errors of the voltages sensors. The process noise covariance matrix can be concluded as follows:

$$Q = diag\ [\dot{x}Noise(1)^2\ \ \dot{x}Noise(2)^2\ \ \dot{x}Noise(3)^2\ \ \dot{x}Noise(4)^2],$$

$$\dot{x}Noise^T = \left[\frac{C}{L_{ss}}\ \ \frac{C}{L_{ss}}\ \ a\ \ 0\right],$$

where C is the standard deviation of uncertainty in control inputs: C= *0.07 volts*, and a is the standard deviation of shaft acceleration noise: a = 0.5 rad/sec^2.

Using the result in (14),

$$\dot{x} = [di_{as}/dt\ \ di_{bs}/dt\ \ d\omega_{rm}/dt\ \ d\theta_{rm}/dt]^T = \begin{bmatrix} -\frac{r_s}{L_{ss}}x(1) + \frac{\psi_m}{L_{ss}}x(3).\sin x(4) + \frac{1}{L_{ss}}u_{as} \\ -\frac{r_s}{L_{ss}}x(2) - \frac{\psi_m}{L_{ss}}x(3).\cos x(4) + \frac{1}{L_{ss}}u_{bs} \\ \frac{\psi_m}{J}[-x(1)\sin x(4) + x(2)\cos x(4)] - \frac{B}{J}x(3) \\ x(3) \end{bmatrix}$$

Consequently, the matrix A can be calculated as follows:

$$A(x,t) = \frac{\partial f(x,u,t)}{\partial x} = \begin{bmatrix} -\frac{r_s}{L_{ss}} & 0 & \frac{\psi_m}{L_{ss}}.\sin x(4) & \frac{\psi_m}{L_{ss}}x(3).\cos x(4) \\ 0 & -\frac{r_s}{L_{ss}} & -\frac{\psi_m}{L_{ss}}.\cos x(4) & \frac{\psi_m}{L_{ss}}x(3).\sin x(4) \\ -\frac{\psi_m}{J}\sin x(4) & \frac{\psi_m}{J}\cos x(4) & -\frac{B}{J} & -\frac{\psi_m}{J}[x(1)\cos x(4) + x(2)\sin x(4)] \end{bmatrix}$$

The simulation results of the EKF variables estimation, in addition to the estimation errors, are depicted in Fig. 3, Fig. 4 and Fig. 5. For analysis purposes, the standard deviation of estimation error for the state vector components was calculated; i.e. root mean square error (RMSE).

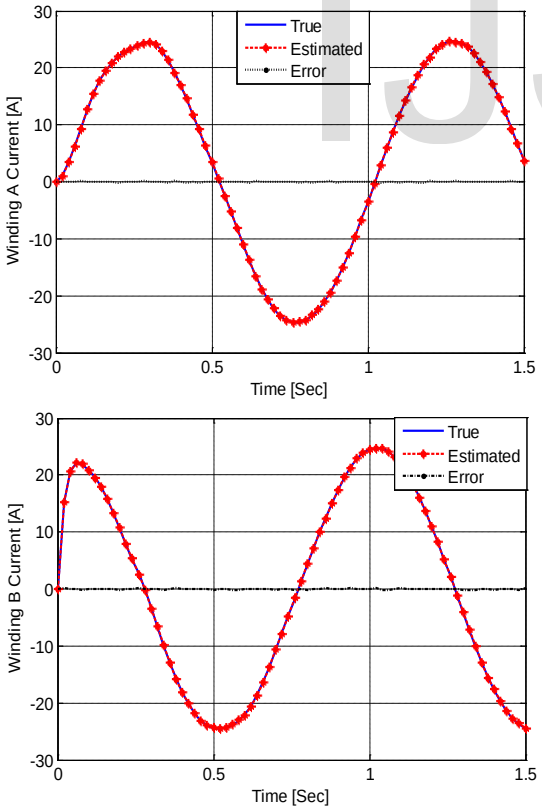

Fig. 3. Motor true and estimated currents.

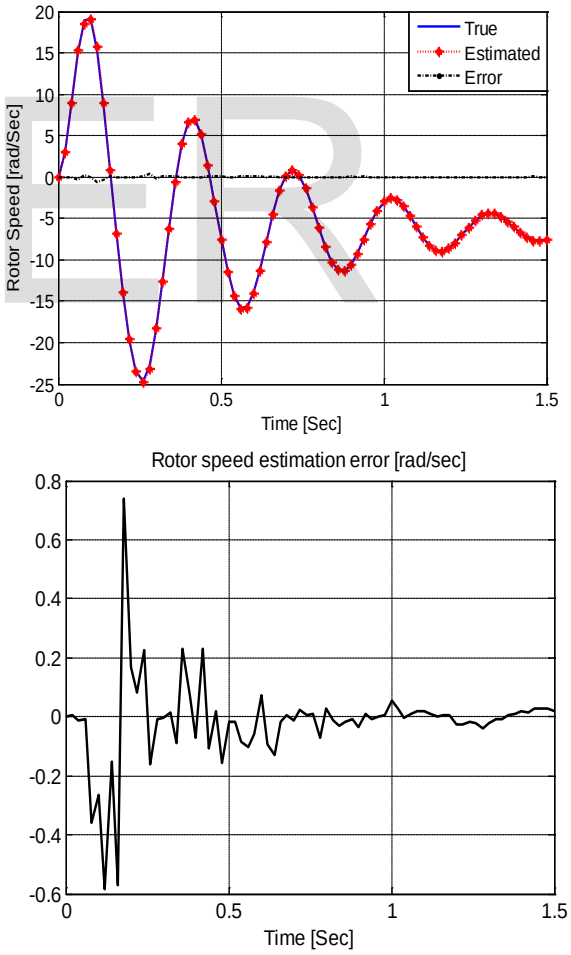

Fig. 4. True and estimated motor speed with estimation errors.

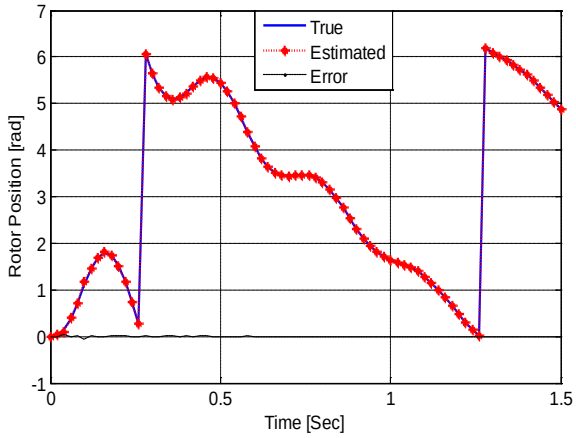

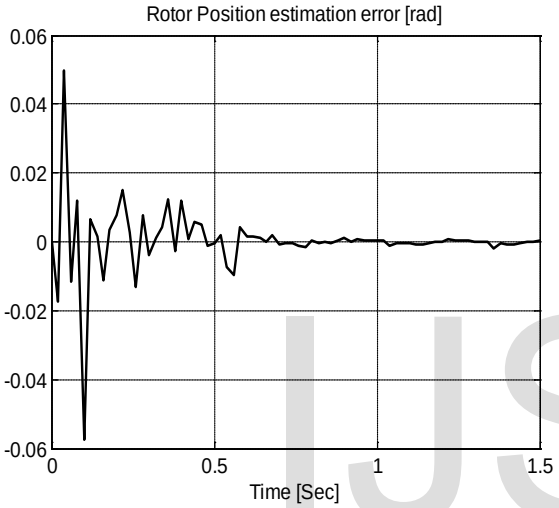

Fig. 5. True and estimated motor's rotor position with estimation errors.

The following observations can be made from the simulation results:

- The stator currents estimation errors remain less than 0.95%.
- The maximum steady-state error between theoretical and estimated rotor position is merely 1%, then after 0.3 sec it becomes less than ±0.2%. While the maximum steady-state error between theoretical and estimated motor speed is about 5% and it decreases to 1% after 0.3 sec.
- The estimated speed could be applied as the feedback signal in the control circuits to achieve sensorless speed control system. Moreover, the important variable to be estimated, which is the rotor position here, was estimated by a standard deviation about 0.001 rad.

The previous observations are confirmed by plotting the *P* matrix trace, as shown in Fig. 6.

The observations extracted from the simulation results; the stator currents, rotor's speed, and rotor's position estimation errors were arranged in Table 3.

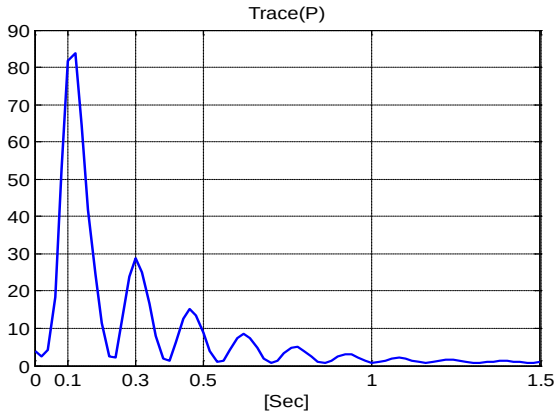

Fig. 6. Covariance matrix of the estimation error.

5 Temprature Change Effects

The temperature of the electric machines changes over a wide range during operation. Since the windings resistance and the permanent magnets material characteristics are functions of temperature, the performance of the machine should be studied in different working temperatures. The influence of these time-varying parameters on the supply voltages is declared in equations set (14).

The considered motor data [11] at temperature 120 °C are shown in Table 2.

TABLE 2
MOTOR DATA AT 120 °C

Parameter	Value
V_{LL}	7.6 [V]
$i_{as_{max}} = i_{bs_{max}}$	7.4 [A]
J	0.0015 [Kg.m^2]
r_s	0.57 [Ω]
L_{ss}	0.011 [H]
ψ_m	0.02 [N.m/A]
B_m	0.005 [N.m.sec / rad]

Again, running the simulation, the motor currents, rotor's speed and position are as illustrated in Fig. 7, Fig. 8 and Fig. 9.

The estimation errors were arranged in Table 3.

TABLE 3
MOTOR VARIABLES ESTIMATION ERRORS

Parameter	σ_e * at T = 20°C	σ_e * at T = 120°C	Steady State error
i_{as}, i_{bs} (A)	0.0980	0.0999	± 0.95 %
ω_r (rad/sec)	0.0235	0.0286	± 1 %
θ_r (rad)	0.0009	0.0019	± 0.1 %

*Standard deviation of estimation error.

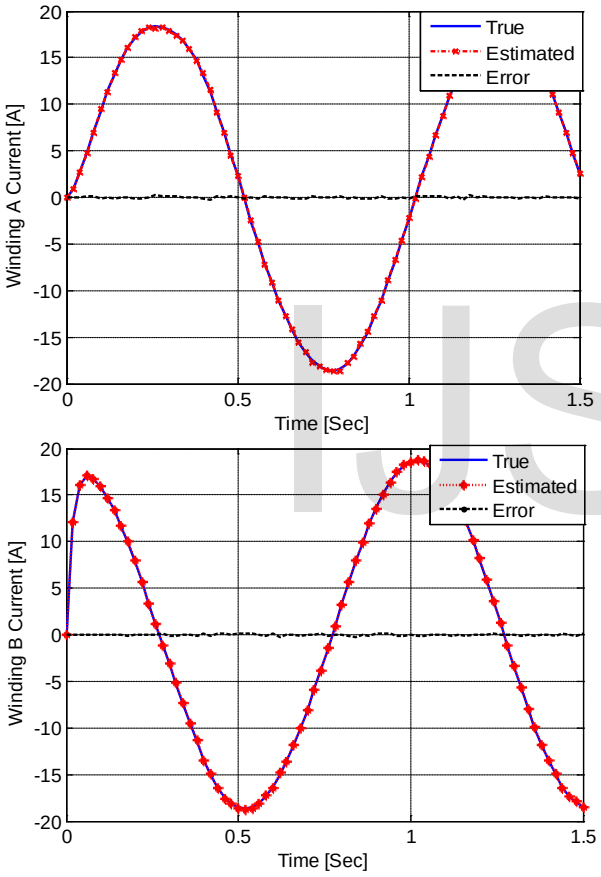

Fig. 7. Motor true and estimated currents at 120 °C.

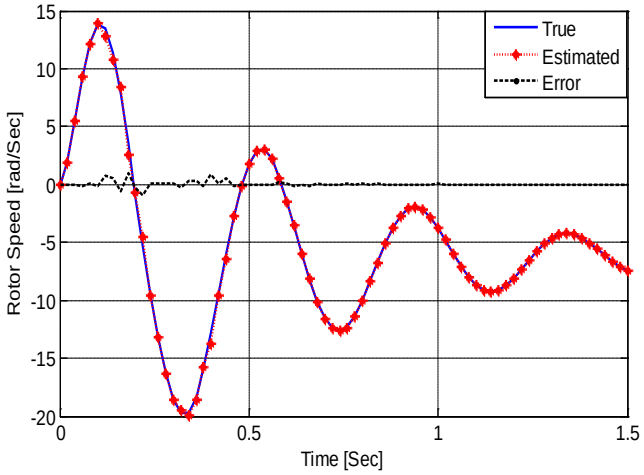

Fig. 8. True and estimated motor speed with estimation errors at 120 °C.

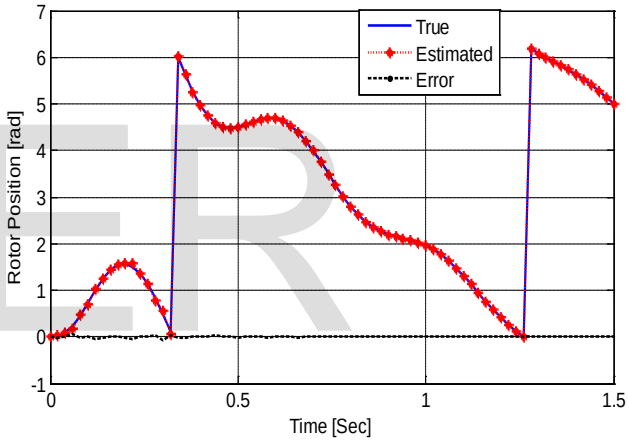

Fig. 9. True and estimated rotor's position with estimation errors at 120 °C.

Analyzing the results, illustrated in last Figures and tabulated in Table 3, leads to the following observations:

- The stator currents of hot motor decreased because the resistances increased.
- The electromagnetic torque generated by the hot motor will decrease because the stator currents decrease and the motor constant ψm also decreased.

$$T_e = RT\psi_m[-i_{as}\sin(RT\theta_{rm}) + i_{bs}\cos(RT\theta_{rm})]$$

6 CONCLUSIONS

A dynamic model of a two-phase stepper motor, besides its Simulink® model, was presented in detail in this paper. In addition, the importance of rotor position measurement for supplying voltage has been clarified. Using the presented method, which applies the EKF, it is possible to estimate the speed and rotor position of the BLDC motor with sufficient

accuracy in both the steady-state and dynamic modes of operation. Thus, the extended Kalman filter is a solution to precisely estimate the state of nonlinear system.

The temperature change effects on the motor's performance were also verified.

NOMENCLATURES

u_{as}, u_{bs}	The phase voltages supplied to the stator windings a_s and b_s
i_{as}, i_{bs}	The phase currents
ψ_{as}, ψ_{bs}	Stator flux linkages per second
r_s	Stator windings resistance
L_{asas} , L_{bsbs}	Self-inductances
L_{asbs}, L_{bsas}	Mutual inductances
θ_r	The rotor angle
ω_r	The rotor angular velocity
RT	The rotor tooth number
T_e, T_L	Electromagnetic and load torques
J	Moment of inertia
$\hat{x}$	Estimated state vector
P	Covariance matrix of estimation error
B_m	Viscous friction coefficient

REFERENCES

[1] R. Marino, P. Tomei, and C.M. Verrelli, *Induction Motor Control Design*. Springer-Verlag London, 2010.

[2] M. Kia, K.R. Rezayieh, and R. Taherkhani, "A Novel Method for Measuring Rotational Speed of BLDC Motors Using Voltage Feedback," *2nd International Conference on Control, Instrumentation and Automation (ICCIA)*, pp. 791-794, December 2011.

[3] W. Kim and C.C. Chung, "Novel Position Detection Method for Permanent Magnet Stepper Motors Using Only Current Feedback," *IEEE Transactions on magnetics*, vol. 47, no. 10, pp. 3590-3593, 2011, doi: 10.1109/TMAG.2011.2144573.

[4] N. Kasa and H. Watanabe, "A Mechanical Sensorless Control System for Salient-Pole Brushless DC Motor with Auto-calibration of Estimated Position Angles," *IEEE Transactions on industrial electronics*, vol. 47, no. 2, pp. 389-395, 2000, doi: 10.1109/41.836354.

[5] R. Dhaouadi, N. Mohan, and L. Norum, "Design and Implementation of an Extended Kalman Filter for the State Estimation of a Permanent Magnet Synchronous Motor , IEEE Power Electronics, vol. 6, no. 3, pp. 491-497, July 1991.

[6] M. Bendjedia, Y. Ait-Amirat, B. Walther, and A. Berthon, "Position Control of a Sensorless Stepper," *IEEE Transactions on power electronics*, vol. 27, no. 2, pp. 578-587, 2012, doi: 10.1109/TPEL.2011.2161774.

[7] A. Masi, M. Butcher, M. Martino, and R. Picatoste, "An Application of the Extended Kalman Filter for a Sensorless Stepper Motor Drive Working with Long Cables," *IEEE Transactions on industrial electronics*, vol. 59, no. 11, pp. 4217-4225, 2012, doi: 10.1109/TIE.2011.2178213.

[8] P.C. Krause, O. Wasynczuk, and S.D. Sudhoff, *Analysis of Electric Machinery and Drive Systems*. IEEE press, 2002.

[9] F.L. Lewis, L. Xie, and D. Popa, *Optimal and robust estimation With an Introduction to Stochastic Control Theory*. CRC press, 2008.

[10] D. Simon, *Optimal State Estimation: Kalman, H∞ and Nonlinear Approaches*. Hoboken, NJ: Wiley, 2006.

[11] S.E. Lyshevski, "Electromechanical Flight Actuators for Advanced Flight Vehicles,"*IEEE Transactions on aerospace and electronic systems*, vol. 35, no. 2, pp. 511-518, 1999, doi: 10.1109/7.766933.

[12] B. Terzic and M. Jadric, "Design and Implementation of the Extended Kalman Filter for the Speed and Rotor Position Estimation of Brushless DC Motor," *IEEE Transactions on industrial electronics*, vol. 48, no. 6, pp. 1065-1073, 2001, doi: 10.1109/41.969385.